Catalysis Today 150 (2010) 22–27

Contents lists available at ScienceDirect

Catalysis Today

journal homepage: www.elsevier.com/locate/cattod

Hydrogenation of chiral nitrile on highly ordered mesoporous carbon-supported Pd catalysts

Xiao-Feng Guo, Yong-Suk Kim, Geon-Joong Kim *

Department of Chemical Engineering, Inha University, 253 Younghyun-dong, Incheon, 402-751, Republic of Korea

ARTICLE INFO

Article history:
Available online 30 May 2009

Keywords:
Mesoporous carbon
Pd catalyst
Hydrogenation
(S)-3-pyrrolidinol

ABSTRACT

A highly ordered mesoporous carbon (C-SBA-15 and C-SBA-16) was synthesized by nanocasting method using its corresponding mesoporous silica (SBA-15 and SBA-16) as a template. The obtained porous carbons have high surface areas, large pore volume and a narrow pore size distribution. The N_2-adsorption data for C-SBA-15 have provided the BET area of 2029 $m^2\,g^{-1}$ and the total pore volume of 1.7 $cm^3\,g^{-1}$, and 1637 $m^2\,g^{-1}$ and 1.1 $cm^3\,g^{-1}$ for C-SBA-16, respectively. The palladium metal impregnated carbon catalysts were employed in the synthesis of (S)-3-pyrrolidinol from chiral (S)-4-chloro-3-hydroxybutyronitrile, and a high yield to (S)-3-pyrrolidinol-salt was obtained by using 1 wt% Pd/C-SBA-16. It was investigated that the well-dispersed Pd metals in the confined mesopores are efficient for the hydrogenation of cyano groups to amine.

1. Introduction

Activated carbon-supported metal catalysts have been commonly used in organic synthesis and fine chemical industry due to their many unique properties, such as high surface area and excellent chemical stability in both acidic and basic media. Activated carbons are highly porous enough to allow the fine dispersion and stabilization of small metallic particles. However, they have a very broad pore size distribution from micro to macroscopic range. Ordered mesoporous carbon (OMC) materials may overcome this obstacle, since they exhibit the large size of pore with a narrow pore size distribution and higher surface areas. In recent years, there was a growing interest in the synthesis of OMCs by using porous inorganic templates as a mold [1–4]. Particularly, the synthesis of OMC that employs ordered mesoporous silicas (OMS) as templates has attracted much attention due to the structural ordering of pores, tailored porosity, and high specific surface area as well as a high stability and easiness of functionalization of the aforementioned mesostructures. These features shed light on future perspectives for the development of new adsorbents [5], catalysts [6], electrode materials [4] and templates for ordered mesoporous inorganic materials [7]. The OMS templates offered a big benefit from the viewpoint of structural order and diversity in achieving novel carbon structures.

We have fabricated OMC replica with a hexagonally ordered mesopore channels, designated as C-SBA-15 and C-SBA-16, by using OMS as a mold in this study. The Pd metal immobilized on those OMC was employed as a catalyst for the synthesis of chiral (S)-3-pyrrolidinol-NaCl by the hydrogenation of (S)-4-chloro-3-hydroxy butyronitrile (Scheme 1). In the catalytic reduction, the effects of support type, Pd-loading amount and reaction time on the yield of product (S)-3-pyrrolidinol-salt were investigated mainly. Pd metal catalysts loaded on OMC having three-dimensionally connected pore channels showed a higher activity than Pd/activated carbon (AC) or OMC with one-dimensional mesopores in that reaction.

2. Experimental

2.1. Synthesis of OMC replica from and OMS template

A high quality SBA-15 was prepared using the triblock copolymer Pluronic P123 (Aldrich) as a surfactant and tetraethylorthosilicate (TEOS, 98%, Aldrich) as a silica source, modifying the synthetic procedure reported by Zhao et al. [8]. The starting composition in molar ratio for the synthesis of high grade SBA-15 was fixed as 1.72 P123:0.1 TEOS:0.6 HCl:20 H_2O. The pure SBA-16 sample was synthesized by using Pluronic F-127 (Aldrich) and TEOS, following the synthetic method reported in the previous paper [9]. The optimum molar ratio was chosen as 1.0 TEOS:0.011 F-127:10.1 ethanol: 0.24 HCl:12 H_2O. C-SBA-15 (CMK-1) was synthesized with silica templates SBA-15 and sucrose as carbon precursor following the procedure in the literature [3,4]. After carbonization in furnace at 80 °C under vacuum, silica template was removed by dissolving with HF solution (50 wt%; Duksan Pure Chemicals Co. Ltd.). The final mesoporous carbon products were

* Corresponding author. Fax: +82 32 872 0959.
E-mail address: kimgj@inha.ac.kr (G.-J. Kim).

0920-5861/$ – see front matter © 2009 Elsevier B.V. All rights reserved.
doi:10.1016/j.cattod.2009.04.022

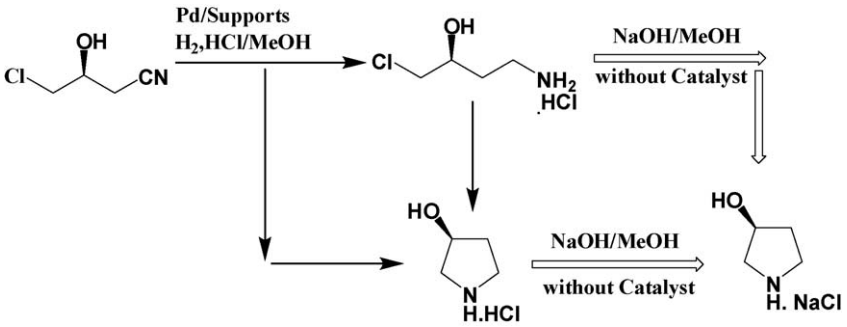

Scheme 1. The synthesis of (S)-3-pyrrolidinol-NaCl salt from chiral (S)-4-chloro-3-hydroxybutyronitrile by hydrogenation.

dried at 100 °C. The C-SBA-16 powder sample was also replicated from SBA-16 silica template by the same procedure mentioned as above.

2.2. Preparation of Pd metal catalysts and determination of metal dispersion

Supported Pd catalysts were prepared by the wetness impregnation of the supports with an aqueous solution containing the desired amount of $Pd(NO_3)^{\bullet}2H_2O$ to yield a final loading of approximately 1.0–5.0 wt% Pd. After impregnation and heating to 80 °C, the suspension was adjusted to pH 10 by adding sodium hydroxide. The Pd/support samples were reduced by adding formaldehyde under the agitation and heating at 80 °C. After further stirring for 2 h, the supported Pd catalysts were collected by filtration and washed with distilled water. The catalysts were dried at 70 °C under vacuum. The carbon monoxide (CO) chemisorption was performed by a dynamic method in once-through flow apparatus equipped with a thermal conductivity detector (TCD). A pulse of CO gas was introduced at 30 °C from a 6-port valve at an interval of 1 min. When the peaks attained a nearly constant area, the adsorption was assumed to reach saturation, and dispersion was calculated. The Pd particle size of Pd/C catalysts was also calculated from CO chemisorption uptakes measured by pulse chemisorption.

2.3. Characterization

X-ray powder diffraction (XRD) data of parent OMS SBA-15 (or SBA-16) and OMC replica (C-SBA-15 and C-SBA-16) were acquired on a D/MAX 2500V/PC diffractometer using Cu Kα radiation. The morphology and microstructures of as-prepared samples were characterized by field emission transmission electron microscopy (FE-TEM, S-4200), and field emission scanning electron microscopy (FE-SEM, JEM-2100F). The nitrogen adsorption/desorption analysis was performed at −196 °C by using a surface area and porosity analyzer equipment (Micromeritics, ASAP 2010). The specific surface areas were calculated according to BET theory, and the mean pore size was determined by BJH analysis.

2.4. Typical procedure for (S)-3-pyrrolidinol-salt

After dissolution of 4 g of (S)-4-chloro-3-hydroxybutyronitrile in 40 mL of methanol, 0.5 mg of 5 wt% palladium-loaded carbon catalyst (Pd/C) and 0.2 mL HCl (35%) were added to that solution. The mixture was stirred under a hydrogen pressure of 1–10 kg/cm^2 at room temperature for 20 h in the autoclave reactor. After filtration of the catalyst from the product mixture, 1.5 g of NaOH was added and the mixture was stirred at room temperature for 2 h. The solvent was evaporated finally to give a (S)-3-pyrrolidinol-NaCl salt. The yield of product was determined from the weight of isolated salt.

3. Results and discussion

The formation of mesopores in C-SBA-15 and C-SBA-16 was determined by XRD, TEM and N_2 adsorption analysis. The ordered arrangement of mesopore in the synthesized OMC replica (C-SBA-15) gives rise to the well-resolved XRD peaks as shown in Fig. 1, which can be assigned to (1 0 0), (1 1 0), and (2 0 0) diffractions of the 1D hexagonal space group (*p6mm*). The mesoporous C-SBA-16 also showed well-resolved Bragg diffraction peaks at 2θ angle below 5°, indicating the presence of mesopore channels. The cubic (*Im3m*) space group was investigated for the SBA-16 sample after calcination. The XRD results showed that the carbon replicas fabricated from OMS in this work exhibited well-developed regular mesoporous channels.

FE-SEM images revealed that as-synthesized C-SBA-15 sample consists of many rope-like domains with relatively uniform sizes of ~2 μm, which are aggregated into wheat-like macrostructures. Both of C-SBA-15 and C-SBA-16 replica have exhibited the same morphological feature as compared to the corresponding parent SBA-16 silica mold. This result indicates that the introduction of sucrose to form the carbon wall was successfully performed in the whole range of mesopores of starting SBA-15 and SBA-16 silica.

Fig. 2 shows the two FE-TEM images of C-SBA-15 viewed along or perpendicular to the direction of hexagonal pore arrangement. As can be seen in those TEM images, the mesopore structure of C-SBA-15 is exactly the inverse replica of SBA-15 silica. The TEM image at high magnifications showed the well-defined mesopore structures

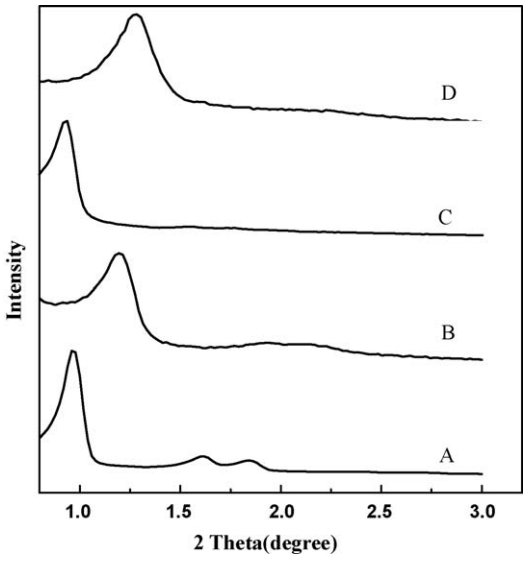

Fig. 1. X-ray diffraction patterns of SBA-15 (A); C-SBA-15 (B); SBA-16 (C); C-SBA-16 (D).

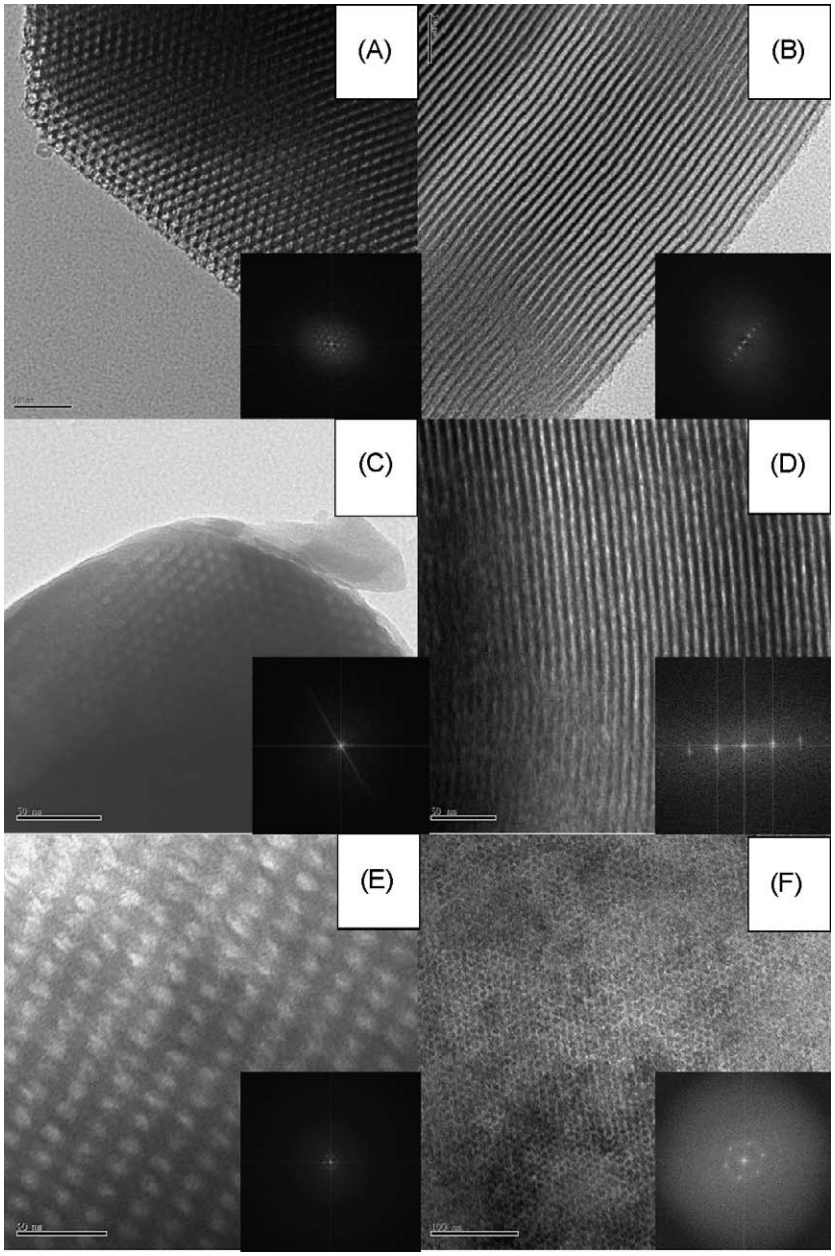

Fig. 2. TEM photographs of SBA-15 along the hexagonal pore arrangement (A); SBA-15 perpendicular to the hexagonal pore arrangement (B); C-SBA-15 along the hexagonal pore arrangement (C); C-SBA-15 perpendicular to the hexagonal pore arrangement (D); SBA-16 (E); C-SBA-16 (F). The electron diffractograms are included in the same photos.

in OMCs. The carbon nanorods are interconnected by spacers, which are constituted by the carbon that filled the channel-interconnecting micropores within the SBA-15 wall [10]. The TEM image and electron diffractogram along [1 1 1] incidence for C-SBA-16 indicated the high structural ordering of the carbon, which means the exact inverse replica of the SBA-16 silica template.

To analyze the pore geometry and structure of OMCs, BJH analyses were performed to measure the N_2 adsorption branch corresponded to the equilibrium (Fig. 3). N_2 adsorption/desorption isotherm of calcined original SBA-15 (Fig. 3A) was the H1-type hysteresis loop that is typical for mesoporous materials with ordered cylindrical channels. Whereas, the mesoporous C-SBA-16 showed a hysteresis curve corresponding to the cage-like mesopore channels (Fig. 3C). The N_2-adsorption data for C-SBA-15 have provided the BET area of 2029 $m^2\ g^{-1}$ and the pore volume of 1.7 $cm^3\ g^{-1}$. The latter can be related to the volume of the ordered mesopores primarily, with minor contribution of micropores. The C-SBA-16 also exhibited a very high adsorption amount of nitrogen relative to the SBA-16 silica template. The C-SBA-16 sample gave the BET area of 1637 $m^2\ g^{-1}$ and the pore volume of 1.1 $cm^3\ g^{-1}$. The N_2 adsorption result also indicates that C-SBA-15 carbon had a quite narrow pore-size distribution of 5.4 nm, while the pore size distribution for SBA-15 silica was centered at 7.2 nm. The mean pore size of C-SBA-16 was 6.1 nm, which was larger by approximately 2 nm than that of SBA-16 silica template (4.3 nm).

The TEM photographs of the Pd metal-loaded OMC are shown in Fig. 4. With the increased loading content of Pd from 1 wt% to 5 wt%, the average diameter of the metal particles was investigated to increase and the aggregates were grown apparently at the outer surface of pores in TEM images. For the impregnation of Pd even at the level of 1 wt%, many isolated particles were investigated on the AC support, relative to OMC.

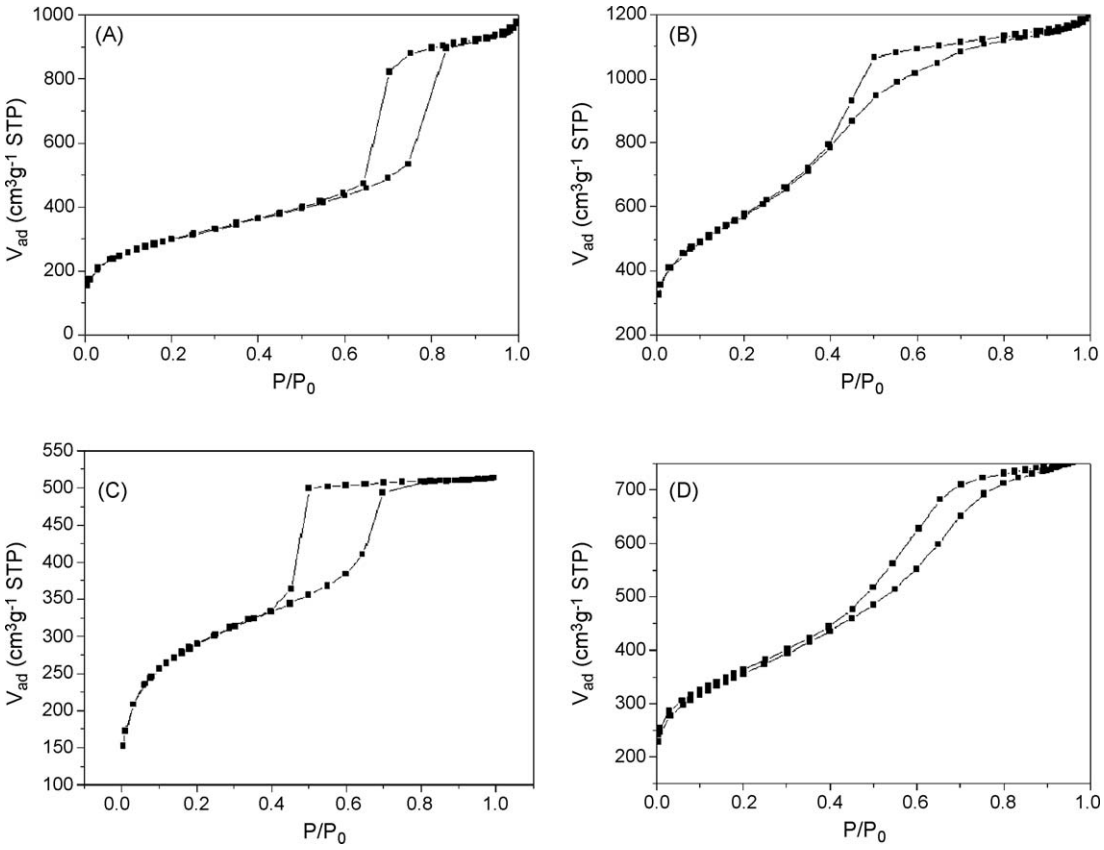

Fig. 3. N_2 adsorption/desorption isotherms for SBA-15 silica (A); C-SBA-15 (B); SBA-16 silica (C); C-SBA-16 (D).

To determine the dispersion of Pd metals on the surfaces of carbon support, the chemisorption of CO was performed, and the obtained results are listed in Table 1. Since it was difficult to distinguish the Pd particles present in the mesopores from the TEM images, the mean metal size of Pd was calculated from the CO adsorption data. The type of support gave a difference in the dispersion of Pd metal. From the chemisorption of CO, smaller size of Pd metal was determined as compared to the observed size in TEM images. However, it is believed that the small size Pd particles were formed mainly inside the mesopore channels of OMCs. Only the Pd particles present at the outer surface of mesopore could be investigated in TEM images (Fig. 4). With an increase of palladium content from 1% to 5%, the average diameter of the palladium particles gradually increased. Higher dispersion of Pd metal was investigated in the cases of C-SBA-15 and C-SBA-16, relative to the active carbon or SBA-15 silica as shown in Table 1.

In the catalytic reduction of the 4-chloro-3-hydroxybutyronitrile, metal catalysts such as Raney metal, palladium and platinum can be used preferably to convert the cyano group into the primary amine. In this work, Pd-containing OMCs were tested as a catalyst for the synthesis of (S)-3-pyrrolidinol-NaCl salt (S-PD-salt) from the optically active (S)-4-chloro-3-hydroxybutyronitrile (S-CHB), and the results for the catalytic activity are listed in Figs. 5–7.

Accordingly the effect of support type on the product yield was determined, and the obtained results are shown in Fig. 5. The loading amount of Pd on the supports was fixed as 5 wt% for all cases. The 5 wt% Pd/C-SBA-16 gave the higher yield to S-PD-salt than the 5 wt% Pd/AC in the reduction of S-CHB. Additionally the catalytic activity was compared by using the parent mesoporous silica. The Pd catalyst supported on SBA-15 silica has resulted in a lower activity than that immobilized over OMC. The larger metal particles were formed on the surfaces of SBA-15 silica support as compared to the carbons (Table 1). In the case of silica support, the different nature of surfaces could also cause the change of reactivity. However, well-dispersed Pd metals in the confined mesopores are efficient for the hydrogenation of cyano groups to amine.

To investigate the dispersion effect of palladium metal particles on the reduction activity in the hydrogenation reaction of S-CHB, 1–5 wt% of Pd-loaded C-SBA-16 catalysts were applied, and the result are shown in Fig. 6. In this case, the total amount of palladium was controlled to be same in the reaction system, respectively. The 1.0 wt% and 3.0 wt% Pd/C-SBA-16 exhibited a higher catalytic activity than 5.0 wt% Pd/C-SBA-16 catalyst. From this result, it is interpreted that the smaller size of Pd formed in the mesopores of C-SBA-16 with relatively high dispersion (Table 1) could accelerate the reduction of the substrate under the same conditions.

The effects of the reaction temperature as well as H_2 pressure were investigated on the yield of S-PD-salt in the reduction of S-CHB, and the obtained result is summarized in Fig. 7. With the increasing hydrogen pressure, the yields of product have increased at the same reaction time. The higher pressure of hydrogen more than 8 bar was not effective for the catalytic reduction. However, under the low H_2 pressure such as 1.0 bar, the reductive reaction has proceeded very slowly. This means that the adsorption of hydrogen on the Pd is important to reduce the substrate. After catalytic reduction of S-CHB, two kinds of product can be formed depending on the reaction condition such as metal types, the reduction temperature and the reaction time, as well as the acidity or basicity in the system. One product is a primary amine salt which is reduced but non-cyclized one, and the other is the cycled (S)-3-pyrrolidinol-HCl salt as shown in Scheme 1. In order to complete the cyclization, it is preferable to conduct the cyclization by further stirring the reduction product under a basic condition to form the cycled S-PD-salt. In this study, higher reaction

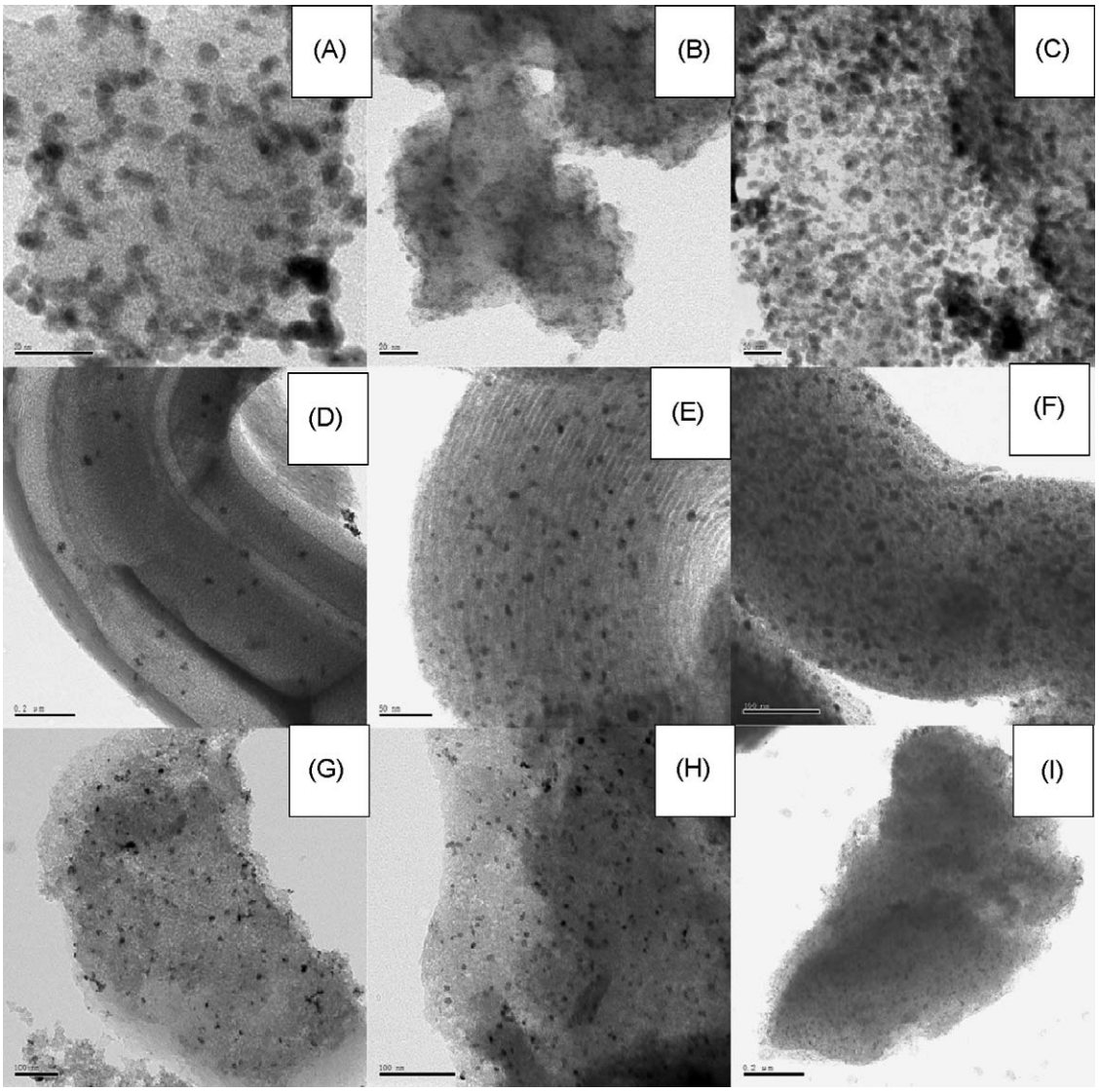

Fig. 4. TEM images of 1 wt% Pd-loaded (A); 3 wt% Pd-loaded (B); 5 wt% Pd-loaded active carbon (C); 1 wt% Pd (D); 3 wt% Pd (E); 5 wt% Pd/C-SBA-15 (F); 1 wt% Pd (G); 3 wt% Pd (H); 5 wt% Pd/C-SBA-16 (I).

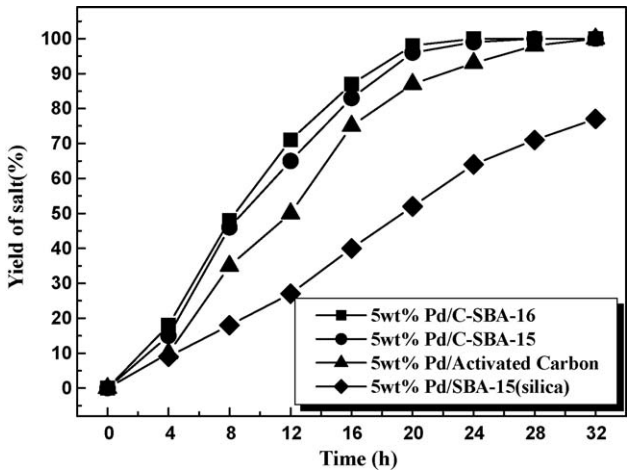

Fig. 5. Catalytic activities of Pd metals loaded on the different type of supports in the hydrogenation of chiral (S)-4-chloro-3-hydroxybutyronitrile to obtain the (S)-3-pyrrolidinol-NaCl salt (H_2 10 atm; temp. 80 °C).

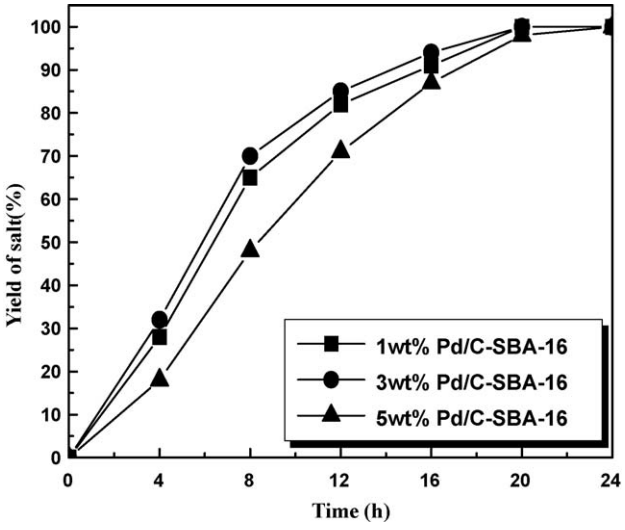

Fig. 6. The effect of Pd-loading amount on the yield of (S)-3-pyrrolidinol-NaCl salt in the hydrogenation of chiral (S)-4-chloro-3-hydroxybutyronitrile by hydrogen (H_2 10 atm; temp. 80 °C: the total palladium amount was controlled to be added as the same amount into the reaction system).

Table 1
Pd particle size of Pd catalysts supported on the carbons.

Catalyst type	Pd particle size by TEM (nm)	Mean Pd metal size (nm)[c]	Pd dispersion (%)[b]	CO uptake (10^{19} molecule CO/g cat.)[a]
1 wt% Pd/C	5.5	5.6	20	1.08
3 wt% Pd/C	8.1	8.0	14	2.36
5 wt% Pd/C	8.8	8.6	13	3.68
1 wt% Pd/SiO_2-SBA-15	6.2	6.0	19	1.01
1 wt% Pd/C-SBA-15	3.9	3.1	36	1.96
3 wt% Pd/C-SBA-15	5.3	3.9	29	4.84
5 wt% Pd/C-SBA-15	6.7	5.1	22	6.23
1 wt% Pd/C-SBA-16	4.4	3.0	37	2.02
3 wt% Pd/C-SBA-16	5.6	3.7	30	5.06
5 wt% Pd/C-SBA-16	6.5	5.4	21	5.86

[a] Error of measurement was ±5% as determined directly.
[b] Based on the total palladium loaded. An assumption of $CO/Pd_s^0 = 1$ was used, where Pd_s^0 is a reduced surface atom of Pd.
[c] Based on $d = (1.12/D)$ nm, where D = fractional metal dispersion.

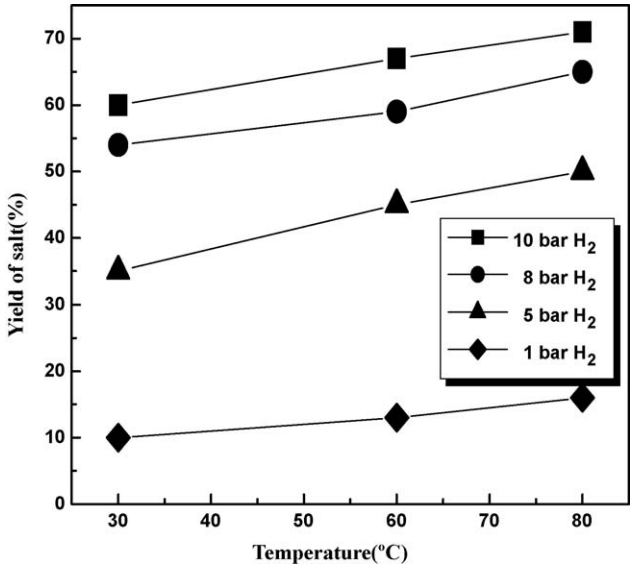

Fig. 7. The effect of reaction temperature and hydrogen pressure on the product yield of (S)-3-pyrrolidinol-NaCl salt (5 wt% Pd/C-SBA-16; reaction time 12 h).

temperature up to 80 °C was essential to obtain the cycled S-PD-salt at the same H_2 pressure. There was a tendency that the cyclization was completed as the reduction time became prolonged.

4. Conclusions

The OMCs such as C-SBA-15 and C-SBA-16 have been synthesized by nanocasting method using their corresponding mesoporous silicas as a mold. The obtained C-SBA-16 has the high surface area with a narrow pore size distribution, exhibiting the BET area of 1637 $m^2\,g^{-1}$ and the total pore volume of 1.1 $cm^2\,g^{-1}$. The Pd metals loaded on the carbon supports were employed in the synthesis of (S)-3-pyrrolidinol-salt from chiral (S)-4-chloro-3-hydroxybutyronitrile. It was investigated that the well-dispersed Pd metals in the confined mesopores are efficient for the hydrogenation of cyano groups to amine, and higher activity was obtained on the Pd/OMCs catalyst than Pd/AC.

References

[1] S.A. Johnson, E.S. Brigham, P.J. Ollivier, T.E. Mallouk, Chem. Mater. 9 (1997) 2448.
[2] T. Kyotani, T. Nagai, S. Inoue, A. Tomita, Chem. Mater. 9 (1997) 609.
[3] R. Ryoo, S.H. Joo, S. Jun, J. Phys. Chem. B 103 (1999) 7743.
[4] J. Lee, S. Yoon, T. Hyeon, S.M. Oh, K.B. Kim, Chem. Commun. (1999) 2177.
[5] T. Ohkubo, J. Miyawaki, K. Kaneko, R. Ryoo, N.A. Seaton, J. Phys. Chem. B 106 (2002) 6523.
[6] S. Han, S. Kim, H. Lim, W. Choi, H. Park, J. Yoon, T. Hyeon, Micropor. Mesopor. Mater. 58 (2003) 131.
[7] A.-H. Lu, W. Schmidt, A. Taguchi, B. Spliethoff, B. Tesche, F. Schuth, Angew. Chem. Int. Ed. 41 (2002) 3489.
[8] D. Zhao, Q. Huo, J. Feng, B.F. Chmelka, G.D. Stucky, J. Am. Chem. Soc. 120 (1998) 6042.
[9] Y.-S. Kim, X.-F. Guo, G.-J. Kim, Top. Catal. 52 (2009) 197.
[10] S.-H. Joo, S.-J. Choi, I. Oh, J. Kwak, Z. Liu, O. Terasaki, R. Ryoo, Nature 412 (2001) 169.